

# A low-profile ultra-wideband circularly polarized antenna array with metasurface

Wei He<sup>1</sup>  | Yejun He<sup>1</sup>  | Sai-Wai Wong<sup>1</sup>  | Long Zhang<sup>1</sup> | Wenting Li<sup>1</sup> | Haixia Cui<sup>2</sup>  | Amir Boag<sup>3</sup>

<sup>1</sup>College of Electronics and Information Engineering, Shenzhen University, Shenzhen, China

<sup>2</sup>School of Physics and Telecommunication Engineering, South China Normal University, Guangzhou, China

<sup>3</sup>School of Electrical Engineering, Tel Aviv University, Tel Aviv, Israel

## Correspondence

Yejun He, College of Electronics and Information Engineering, Shenzhen University, Shenzhen 518060, China. Email: heyejun@126.com

## Funding information

National Natural Science Foundation of China, Grant/Award Numbers: 62071306, 61801299, 61871433; Mobility Program for Taiwan Young Scientists, Grant/Award Number: RW2019TW001; Shenzhen Science and Technology Program, Grant/Award Numbers: GJHZ20180418190529516, JSGG20210420091805014, JCYJ20200109113601723; Natural Science Foundation of Guangdong Province, Grant/Award Number: 2018A0303130141

## Abstract

In this article, a low-profile ultra-wideband (UWB) circularly polarized (CP) antenna array with metasurface is presented. The antenna array consists of a  $2 \times 2$  polarization conversion metasurfaces (PCMs) and a sequential feeding network. The PCM is composed of  $4 \times 4$  polarization conversion unit-cells. The unit-cell is obtained by putting an ellipse patch into a rectangular ring, connecting the ellipse and the ring with two stubs, and then rotating it by  $45^\circ$ . A linear polarization (LP) slot antenna with a PCM can achieve a CP antenna, which has an impedance bandwidth of about 33.8% (5.4-7.6 GHz) of  $|S_{11}| < -10$  dB and a 3-dB axial ratio (AR) bandwidth of about 24.8% (5.8-7.3 GHz), respectively. The UWB CP characteristics can be achieved when a UWB sequential feeding network is added to the  $2 \times 2$  PCMs. Simulated and measured results show that the proposed antenna array has an impedance bandwidth of about 117% (1.75-6.75 GHz) of  $|S_{11}| < -10$  dB and a 3-dB axial ratio (AR) bandwidth of about 105.7% (2.24-7.35 GHz), respectively. The usable bandwidth can reach 100.3% (2.24-6.75 GHz). Besides, the proposed antenna array achieves a higher gain compared to the traditional slot array and the peak gain of 12.5 dBic at 6 GHz. The overall size of the antenna is  $0.6\lambda \times 0.6\lambda \times 0.03\lambda$  ( $\lambda$  refers to the wavelength of the lowest operating frequency in free space). The proposed antenna array can be widely applied to various wireless communication systems.

## KEYWORDS

circularly polarized antenna, metasurface, ultra-wideband antenna

## 1 | INTRODUCTION

In various wireless communication systems, circularly polarized (CP) antenna have many advantages over the linearly polarized (LP) counterparts, such as improving the polarization mismatch between transmitting and receiving antennas, and reducing multi-path interferences or fading.<sup>1</sup> As multi-functional systems and miniaturized systems become more and more popular, the demand for compact broadband or ultra-wideband

(UWB) antennas is also increasing. A variety of different wideband and UWB CP antennas have been reported.<sup>2-10</sup> A cross dipole with wide open end<sup>2</sup> or elliptical arm<sup>3</sup> can achieve a 3-dB axial ratio (AR) bandwidth of 27% and 96.6%, respectively. A wideband CP dielectric resonator antenna with a partially reflective surface is mentioned in Reference 4, which can obtain 54.9% 3-dB AR bandwidth. A wideband inverted-S dipole antenna with the AR bandwidth of 47% and an UWB asymmetric-S antenna with the AR bandwidth of 84.8% are described

in Reference 5 and Reference 6, respectively. In Reference 7, four broadband CP monopole elements with sequentially rotated feeding network are used to excite UWB CP radiation. An UWB CP reflectarray is proposed in Reference 8, which uses a quasi-I-shaped multi-resonance phasing element to obtain a 3-dB AR bandwidth of about 75%. An UWB CP antenna with four pairs of semicircular patches and four supporting PCBs is illustrated in Reference 9. Its AR bandwidth is about 88.9%. A pair of curved tapered slots with a meshed reflector are used to get 3-dB AR bandwidth of about 84%.<sup>10</sup> Although these antennas can achieve wideband or UWB CP radiation, there is an air-gap between the radiator and the reflector, resulting in a relatively higher profile, which is not well-suited for integration with RF circuits.

Printing a monopole antenna and a modified ground with a slot on the upper and lower surfaces of a single substrate can realize wideband or UWB CP radiation. A G-shaped parasitic strip monopole antenna with defect ground is illustrated in Reference 11, where the AR bandwidth is about 53.9%. When an L-shaped radiator replaces the G-shaped strip, the AR bandwidth can reach 115.2%.<sup>12</sup> Although these antennas have achieved wideband CP

radiation and only have one layer substrate, they all have bidirectional radiation and lower gain. Furthermore, a simple CP patch antenna or an array with a metasurface can also expand the AR bandwidth of the antenna.<sup>13-15</sup> A simple narrow bandwidth modified patch with a symmetrical square ring metasurface is presented in Reference 13. The surface waves propagating along the metasurface is effectively excited to expand the operation bandwidth. A  $2 \times 2$  metasurfaces covered CP patch antennas fed by a sequential-phase network and a CP antenna array where the element is based on a truncated corner and a periodic patch are proposed in Reference 14 and Reference 15, respectively. However, the size of these antennas is relatively larger.

In recent years, the integration of linearly polarized (LP) slot antennas with polarization conversion metasurfaces (PCMs) to generate CP radiation has attracted much attention, due to their low profile, easy implementation in wideband CP arrays, and convenient integration with RF circuits. A PCM consisting of a simple corner-cut square loaded to a slot antenna is presented in Reference 16, and this antenna can obtain a 3-dB AR bandwidth of about 20.6%. By replacing the corner-cut square with an arrow-shaped patch and rotating it  $45^\circ$  to obtain another CP antenna, the

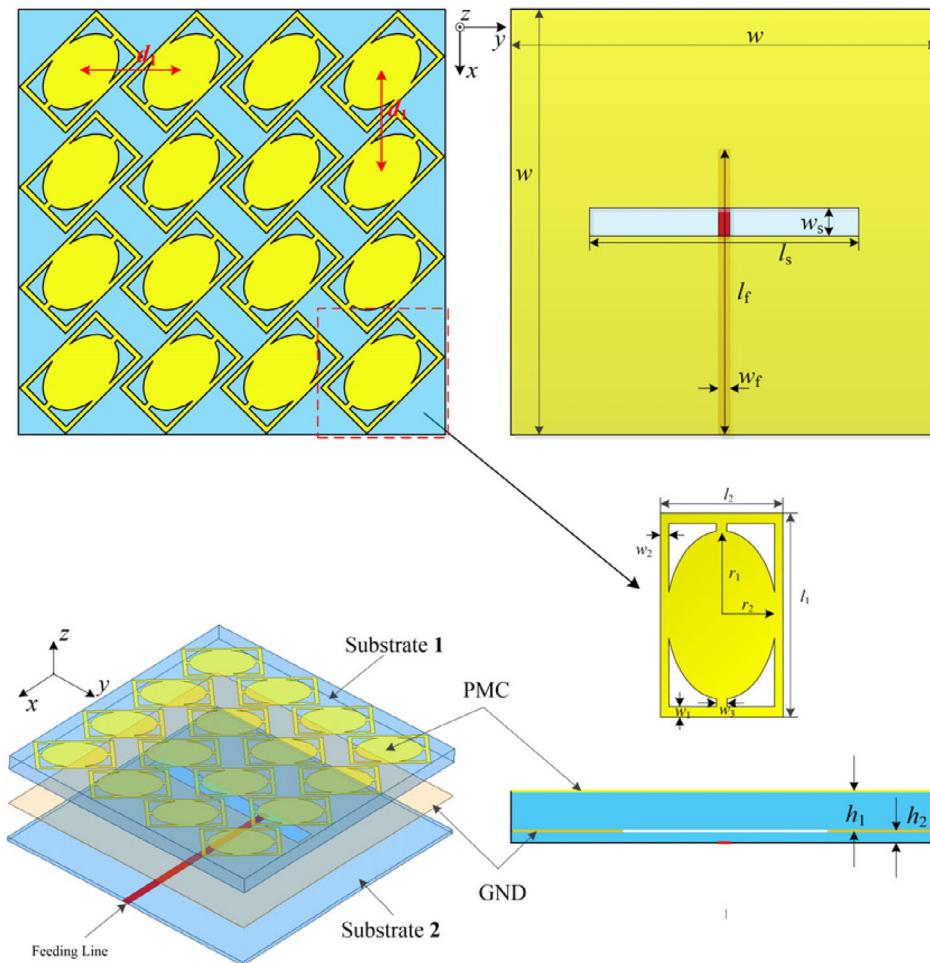


FIGURE 1 Structure of the antenna array element.  $w = 38$  mm,  $l_f = 25.5$  mm,  $l_s = 24$  mm,  $l_1 = 9.7$  mm,  $l_2 = 5.8$  mm,  $w_f = 1$  mm,  $w_s = 2.5$  mm,  $w_1 = 0.5$  mm,  $w_2 = 0.4$  mm,  $w_3 = 0.5$  mm,  $h_1 = 3.7$  mm,  $h_2 = 0.508$  mm,  $d_1 = 9$  mm

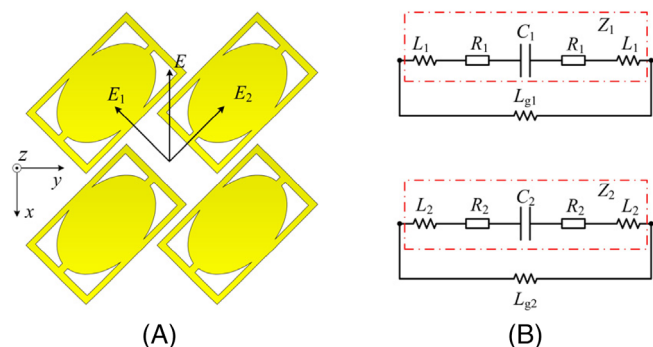


FIGURE 2 (A) Four unit-cells; (B) the equivalent circuit model of the new unit-cell

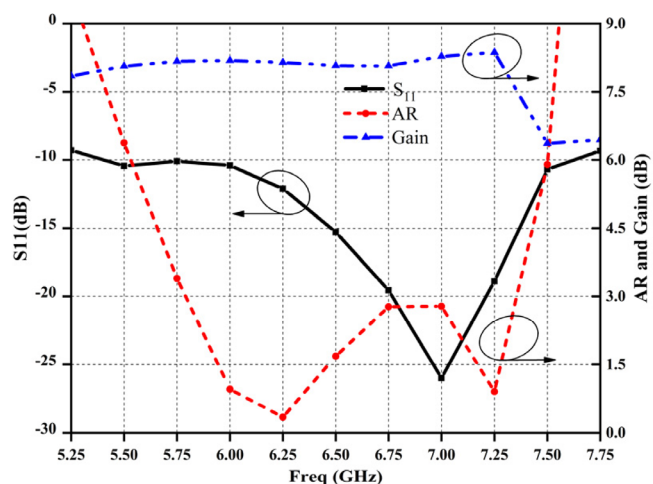


FIGURE 3 Simulated performance of the antenna array element

operating bandwidth is slightly changed to about 18.2%.<sup>17</sup> While the unit-cell of the PCM consists of square and L-shaped patches separated by an L-shaped slot, the AR bandwidth of the antenna can reach 26.2%.<sup>18</sup> In Reference 19, using a simple ellipse patch as the unit-cell of PCM, CP radiation can also be excited, and its AR bandwidth is about 17.4%. To further improve the performance of these antennas, a  $2 \times 2$  antenna array with PCMs can be used. A metasurface-inspired CP antenna array mentioned in Reference 20 has two shorting pins added along the diagonal of the patch to realize the conversion of the polarization, which can obtain AR bandwidth about 26.3% and a peak gain of 13.5 dBi. In Reference 21, a low-profile CP antenna array with polarization conversion electromagnetic band-gap metasurfaces is proposed. The AR bandwidth of this antenna array is about 22.5% and the peak gain reaches 13 dBi. However, all the CP antennas formed by the PCM loaded slot antennas mentioned in earlier works have narrow bandwidth. Therefore, it is difficult to design a low-profile UWB circularly polarized antennas with PCMs.

In this work, a low-profile ultra-wideband (UWB) circularly polarized (CP) antenna array with a metasurface is proposed. Firstly, a PCM composed of  $4 \times 4$  polarization conversion unit-cells is designed. The unit-cell is obtained by putting an ellipse patch into a rectangular ring, connecting the ellipse and the ring with two stubs, and then rotating it by  $45^\circ$ . A simple LP slot antenna covered by the PMC is turned into a CP antenna radiation element. The impedance bandwidth of  $|S_{11}| < -10$  dB is about 33.8% (5.4–7.6 GHz) and the 3-dB AR bandwidth is about 24.8% (5.8–7.3 GHz). Then, an UWB CP antenna array can be constructed by

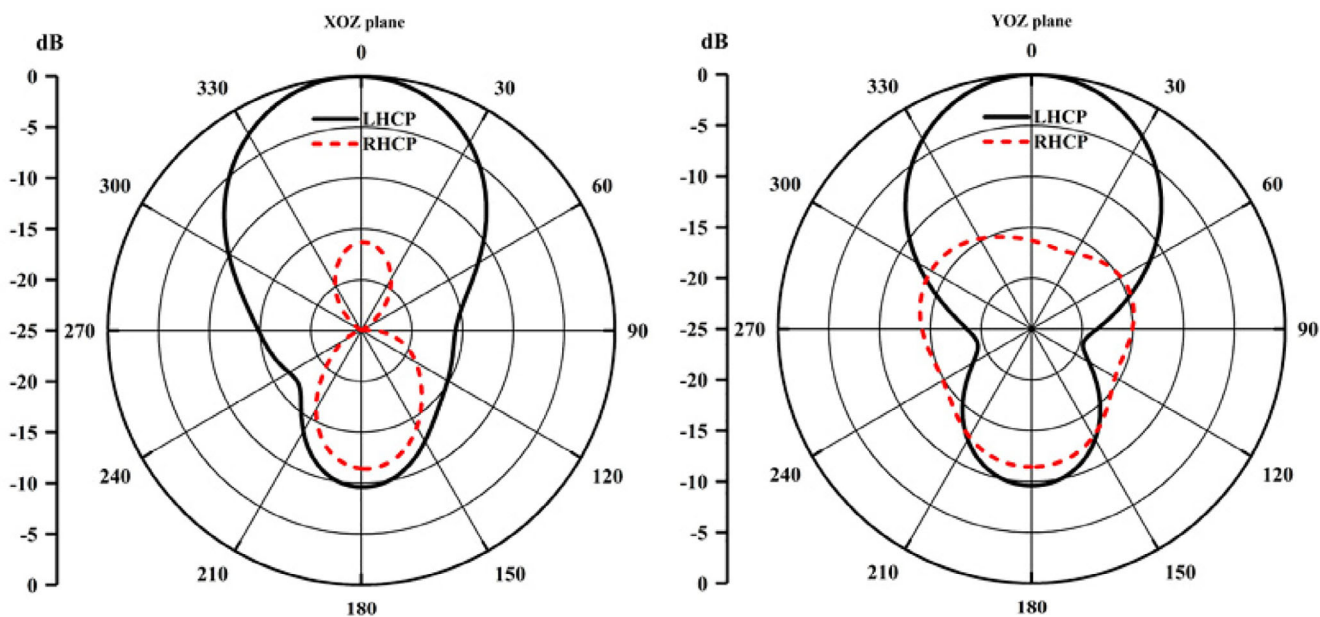


FIGURE 4 Simulated radiation pattern of the antenna array element

using a  $2 \times 2$  arrangement of such elements and an UWB sequential feeding network. The measured result shows that the proposed antenna array has an impedance bandwidth of about 117% (1.75-6.75 GHz) and AR bandwidth of about 105.7% (2.24-7.35 GHz), respectively. Finally, the fabrication and measurement of the proposed UWB CP antenna array verified the design mechanism. Benefiting from the advantages, such as low profile and ultra-wide operating bandwidth, the proposed antenna array with metasurfaces has a wide range of potential applications in wireless communication systems.

## 2 | ANTENNA DESIGN AND ANALYSIS

### 2.1 | The antenna array element

Figure 1 shows the configuration of the proposed antenna array element, which consists of a PCM, a ground plane with a slot, a feeding line, and two layers of substrate. Substrate 1 is F4BM ( $\epsilon_1 = 2.2$ ,  $\tan \delta_1 = 0.004$ ) with a thickness of  $h_1$  and substrate 2 is Rogers 4003 ( $\epsilon_2 = 3.55$ ,  $\tan \delta_2 = 0.0027$ ) with a thickness of  $h_2$ . It

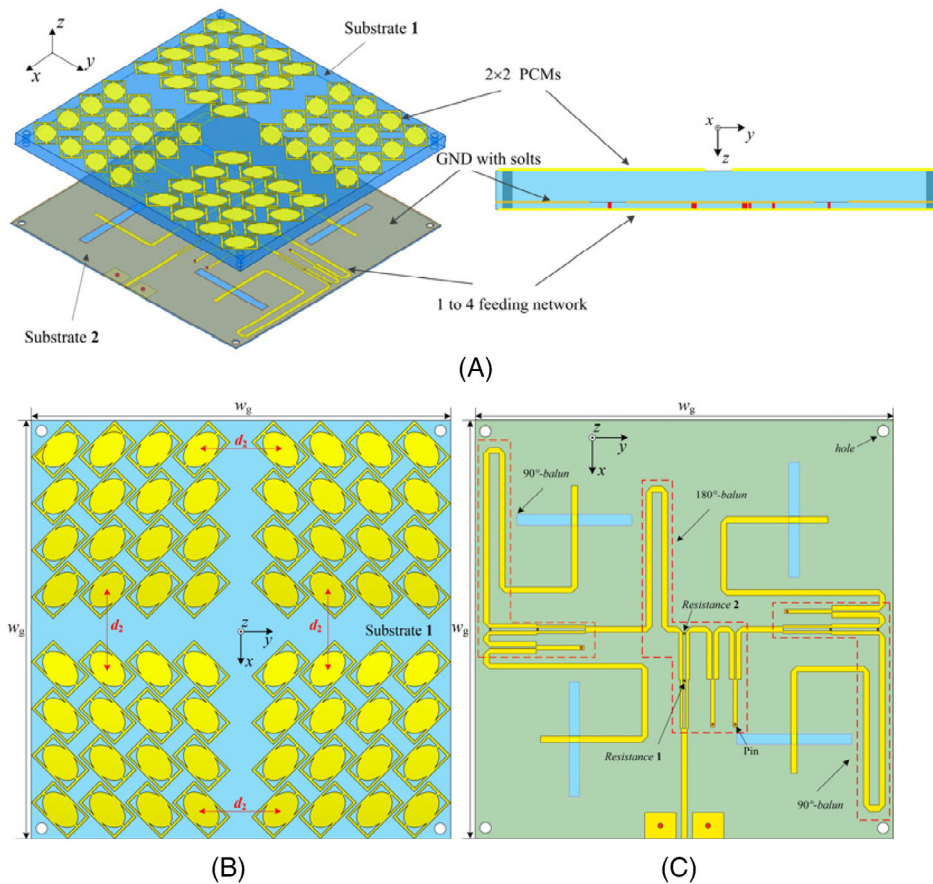


FIGURE 5 The geometry of the proposed antenna array. (A) 3D view and side view; (B) top view; (C) bottom view.  $w_g = 80$  mm,  $d_2 = 13$  mm

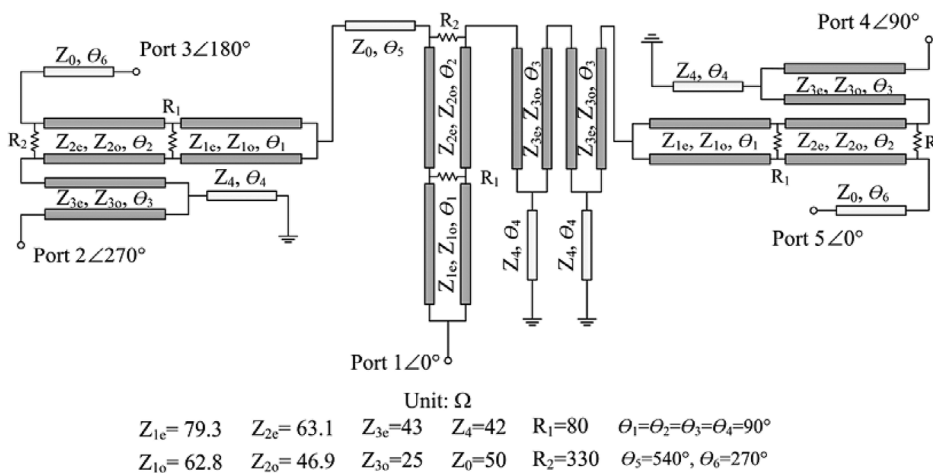


FIGURE 6 Schematic for the feeding network

should be noted that there is only ground plane and no air gap between the two substrates, which results in a low profile antenna structure. As shown in Figure 1, the PCM is composed of  $4 \times 4$  polarization conversion unit-cells. The unit-cell is obtained by putting an elliptical patch into a rectangular ring, connecting the ellipse and the ring with two stubs, and then rotating it by  $45^\circ$ . The LP wave excited by the slot becomes a CP wave after passing through the PCM. How the proposed PCM converts LP wave into CP wave as shown in Figure 2. First, the slot antenna generates an x-direction electric field ( $E$ ), and it can be split into two orthogonal electric field components ( $E_1$  and  $E_2$ ). Consider the new super-cell in the Figure 2(A), when the two electric field components pass through the PCM, the electromagnetic waves will interact with the PCM. The equivalent circuit models for the two electric field components are shown in the

Figure 2(B). This interaction can be expressed by the impedance equations.

$$Z_1 = R_1 + j\omega L_1 + 1/(j\omega C_1) \quad (1)$$

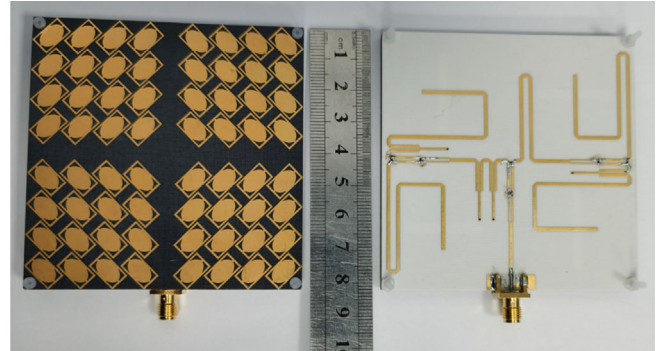


FIGURE 8 Prototype of the proposed antenna array

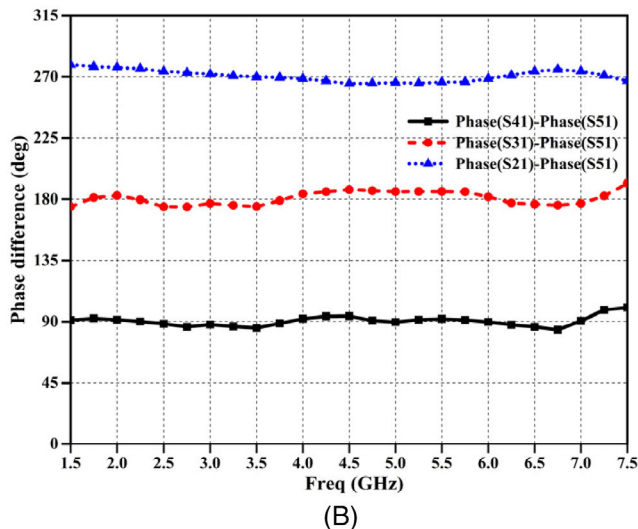
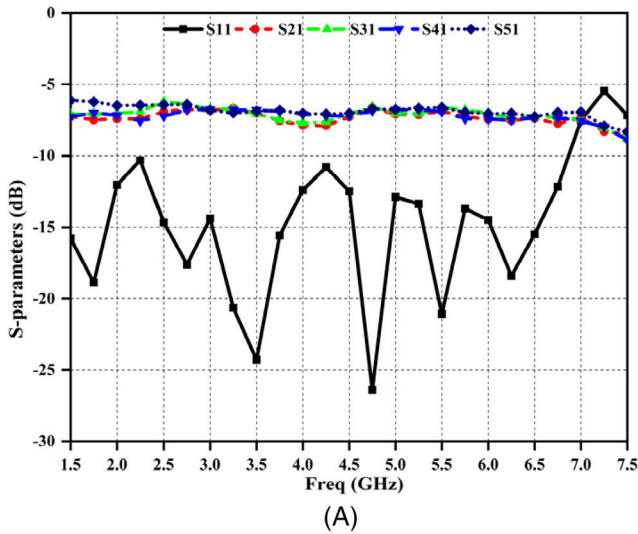


FIGURE 7 Simulated results of the feeding network. (A) S-parameters; (B) phase difference of these four ports

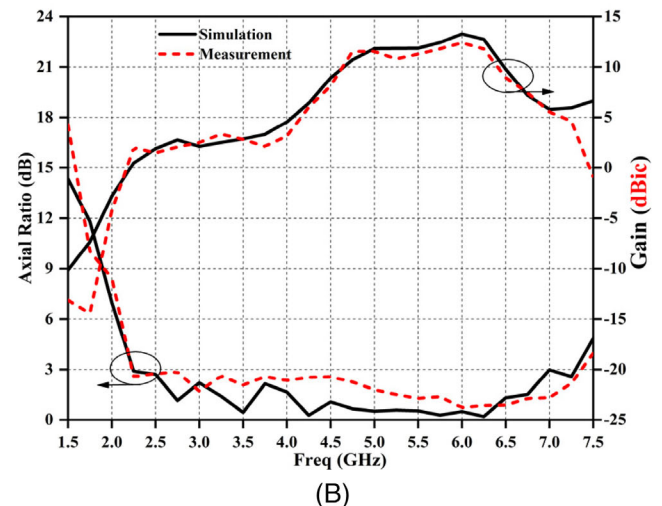
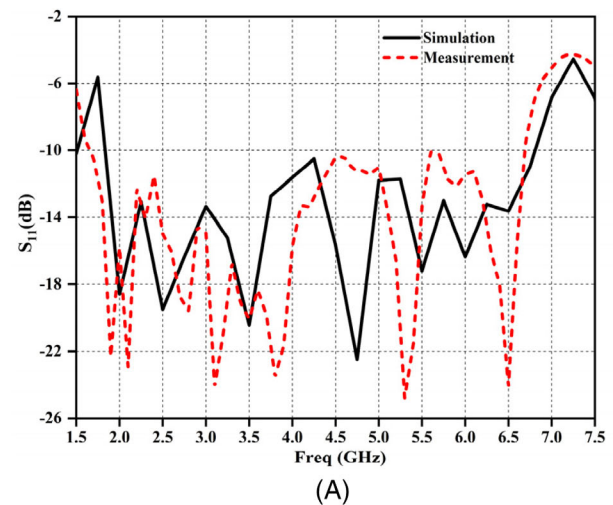


FIGURE 9 Simulated and measured results of the proposed antenna array. (A)  $|S_{11}|$ ; (B) axial ratio and gain

$$Z_2 = R_2 + j\omega L_2 + 1/(j\omega C_2) \quad (2)$$

where  $R_1$ ,  $R_2$ ,  $L_1$ ,  $L_2$ ,  $C_1$ ,  $C_2$  are the resistances, inductances, and capacitances of the unit-cell in Figure 2. These are affected by the structure of the unit-cell. When  $|Z_1| = |Z_2|$  and  $\text{ang}(Z_1) - \text{ang}(Z_2) = \pm 90^\circ$  are satisfied, CP radiation can be generated. The radiation and return loss characteristics of the antenna array element with optimized parameters are shown in Figure 1. The simulation results for  $S_{11}$ , AR, and gain for the antenna array element are shown in Figure 3. The simulated impedance bandwidth of  $|S_{11}| < -10$  dB is about 33.8% (5.4–7.6 GHz), the 3-dB AR bandwidth is about 24.8% (5.8–7.3 GHz), and the average gain in the operating bandwidth is 8.2 dBi. Figure 4 illustrates the radiation pattern of the antenna array element at 6.5 GHz in  $XOZ$  and  $YOZ$  planes. The LHCP radiation is obtained in both  $XOZ$  and  $YOZ$  planes, and the antenna has nearly symmetric radiation patterns in the two planes.

## 2.2 | $2 \times 2$ antenna array with metasurface

Although the single slot antenna loaded with a PCM element has achieved a good CP performance, it also has certain shortcomings, which limit its applications in practice. According to the previous analysis, the operating bandwidth of the antenna element from 5.8 to 7.3 GHz is only about 24.8%. To expand the bandwidth, a  $2 \times 2$  antenna array is designed. Figure 5 shows the configuration of the

proposed antenna array. Figure 5(A) gives the 3D view and side view of this antenna array. As shown, the antenna array consists of a metasurface, a ground plane with four slots, an UWB feeding network, and two layers of substrate. The material and thickness of the two substrate layers are the same as of the antenna array element. As shown in Figure 5(B), in the  $2 \times 2$  arrangement, the sequentially rotated PCMs are printed on the top surface of substrate 1. The UWB 1 to 4 feeding network is printed on the bottom surface of substrate 2, as shown in Figure 5(C). The schematic of the proposed feeding network is shown in Figure 6. This feeding network having an UWB power divider and stable phase difference performance, and consists of a  $180^\circ$  out-of-phase balun and two  $90^\circ$  baluns, which have been designed in Reference 22. The simulation results of this feeding network are illustrated in Figure 7 (A),(B). The impedance bandwidth of the feeding network with  $S_{11} < -10$  dB is from 1.5 to 6.8 GHz (127.7%), and the phase difference between Port 5 and Port 4, Port 3, Port 2 is maintained at about  $90^\circ$ ,  $180^\circ$ ,  $270^\circ$  within the bandwidth 1.5 to 7.5 GHz, respectively. The magnitude unbalance of the insertion loss is less than 1.5 dB.

## 3 | SIMULATION AND MEASUREMENT RESULTS

To validate the above analysis, the proposed UWB CP antenna array with metasurfaces has been fabricated and measured. The photos of the fabricated antenna are

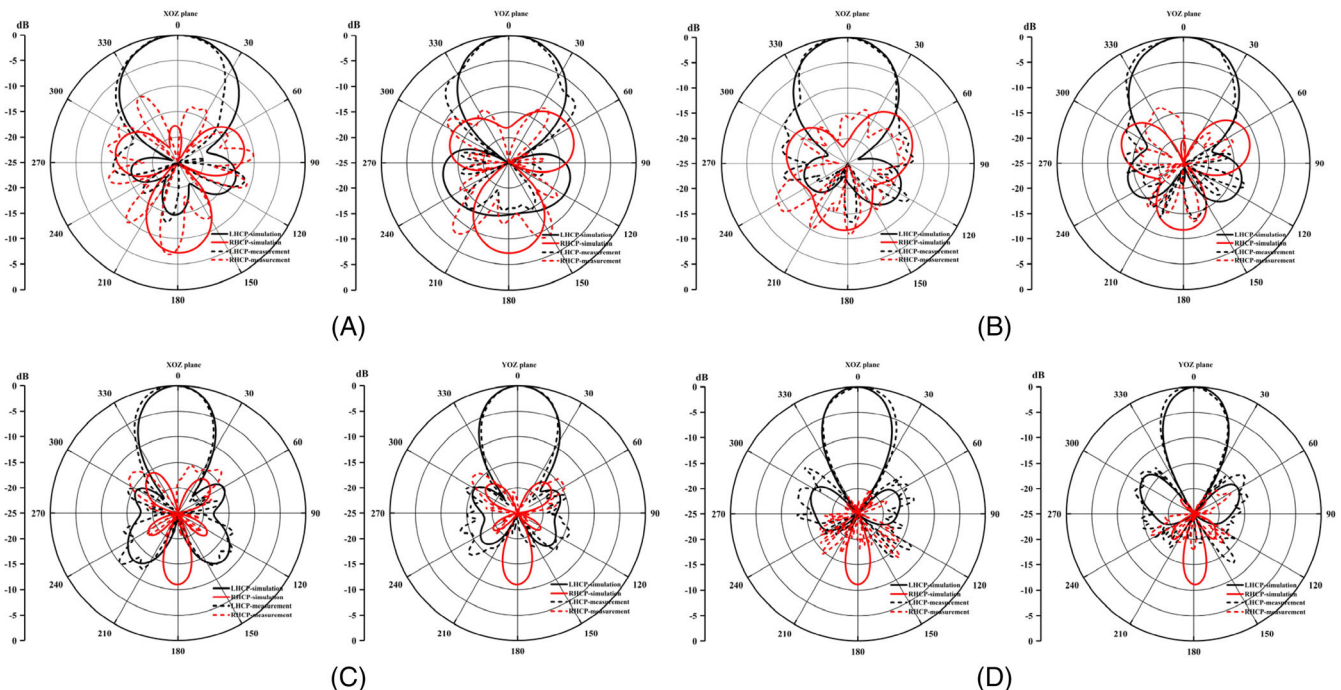


FIGURE 10 Simulated and measured radiation pattern of the proposed antenna array at, (A) 3 GHz; (B) 4 GHz; (C) 5 GHz; (D) 6 GHz

TABLE 1 Comparison between proposed work and previous designed antennas. ( $\lambda$  is the wavelength of the lowest operating frequency)

Ref.	Overall size ( $\lambda^3$ )	Type	Impedance bandwidth (%)	Axial ratio bandwidth (%)	Peak gain (dBi)	Efficiency
6	$1.44 \times 1.44 \times 0.29$	Single asymmetric S-dipole	70.2	84.8	9.55	0.92
8	$\Phi 1.17 \times 0.1$	$2 \times 2$ monopole array	132.8	92.5	12.6	0.6
9	$0.55 \times 0.55 \times 0.12$	$2 \times 2$ semi-circular array	103	89	11	NA
10	$1.21 \times 1.21 \times 0.11$	Curved slot with mesh reflector	99	84	9.6	0.8
12	$0.42 \times 0.38 \times 0.004$	L-shaped radiator with modified ground	124	115	4.5	NA
14	$1.26 \times 1.26 \times 0.046$	$2 \times 2$ patch array with metasurface	41.6	37.3	12	0.88
20	$2.06 \times 2.06 \times 0.08$	$2 \times 2$ slot array with PCMs	32.6	26.3	13.5	NA
21	$1.81 \times 1.81 \times 0.05$	$2 \times 2$ slot array with PCMs	37.3	22.5	13	0.8
22	$1.13 \times 1.13 \times 0.15$	$2 \times 2$ patch array	98	96.3	9.5	0.88
Prop.	$0.6 \times 0.6 \times 0.03$	$2 \times 2$ slot array with PCMs	117	105.7	12.5	0.91

shown in Figure 8. The simulation and measurement results of  $|S_{11}|$ , AR, and gain are shown in Figure 9(A), (B), respectively. The measured impedance bandwidth of  $|S_{11}| < -10$  dB is about 117% (1.75-6.75 GHz), which is a slight shift to the lower frequency compared with the simulation result. As shown in Figure 9(B), the measured 3-dB AR bandwidth can cover the frequency range from 2.24 to 7.35 GHz, reaching 105.7%, which is in agreement with the simulation result. In addition, the measured gain is positive in the operating bandwidth, and slightly lower than the simulated gain, and the peak gain is 12.5 dBi at 6 GHz. Figure 10 describes the measured and simulated results of the radiation pattern at 3, 4, 5, and 6 GHz. As shown in Figure 10, the measured radiation patterns are in good agreement with the simulated results in the upper hemisphere region at 4, 5, and 6 GHz, while the results at 3 GHz in the upper hemisphere region are a little different. Due to the influence on the insertion loss and scattering of the turntable and the coaxial cable used in the tests, the measured results of the back hemisphere have deviated slightly from simulated results. The performance comparison between the proposed antenna and other UWB CP antennas are shown in Table 1. It can be seen that the proposed antenna not only has a smaller size, but also has a wider 3-dB AR bandwidth and a higher gain.

## 4 | CONCLUSION

Using the PCM as a radiation structure loading a simple LP slot antenna can produce a CP antenna. By sequentially rotating  $2 \times 2$  PCMs and slots, and adding an UWB sequential feeding network, a low-profile CP antenna is obtained. The impedance bandwidth and AR bandwidth of the proposed antenna is about 117% (1.75-6.75 GHz) and 105.7% (2.24-7.35 GHz), respectively. Conclusively, this antenna array is a good potential candidate for various UWB applications.

### ORCID

Wei He  <https://orcid.org/0000-0002-0519-0590>

Yejun He  <https://orcid.org/0000-0002-8564-5355>

Sai-Wai Wong  <https://orcid.org/0000-0001-5363-1576>

Haixia Cui  <https://orcid.org/0000-0001-8489-9700>

### REFERENCES

- Wu Q-S, Zhang X, Zhu L. Co-design of a wideband circularly polarized filtering patch antenna with three minima in axial ratio response. *IEEE Trans Antennas Propag.* 2018;66(10):5022-5030.
- He Y-J, He W, Wong H. A wideband circularly polarized cross dipole antenna. *IEEE Antennas Wirel Propag Lett.* 2014;13:67-70.

3. Zhang L, Gao S, Luo Q, et al. Single-feed ultra-wideband circularly polarized antenna with enhanced front-to-back ratio. *IEEE Trans Antennas Propag.* 2016;64(1):355-360.
4. Wen J, Jiao Y-C, Zhang Y-X, et al. Wideband circularly polarized dielectric resonator antenna loaded with partially reflective surface. *Int J RF Microw Comput Aided Eng.* 2019;29:e21962.
5. Zhang L, Gao S, Luo Q, Young PR, Li W, Li Q. Inverted-S antenna with wideband circular polarization and wide axial ratio beamwidth. *IEEE Trans Antennas Propag.* 2017;65(4):1740-1748.
6. He W, Zhang L, He Y-J, et al. An ultra-wideband circularly polarized asymmetric-S antenna with enhanced bandwidth and beamwidth performance. *IEEE Access.* 2019;7:134895-134902.
7. Xu R, Gao S, Liu J, et al. Analysis and design of ultrawideband circularly polarized antenna and array. *IEEE Trans Antennas Propag.* 2020;68(12):7842-7853.
8. Guo W-L, Wang G-M, Liu K-Y, Zhuang YQ, Ge QC. Design of single-layered ultrawideband high-efficiency circularly polarized reflectarray. *IEEE Antennas Wirel Propag Lett.* 2018;17(8):1386-1390.
9. Tan W-H, Shan X-Y, Shen Z-X. Ultra-wideband circularly polarized antenna with shared semicircular patches. *IEEE Trans Antennas Propag.* 2021;69(6):3555-3559.
10. Pan Y-S, Dong Y-D. Low-profile low-cost ultra-wideband circularly polarized slot antennas. *IEEE Access.* 2019;7:160696-160704.
11. Midya M, Bhattacharjee S, Mitra M. Broadband circularly polarized planar monopole antenna with G-shaped parasitic strip. *IEEE Antennas Wirel Propag Lett.* 2019;18(4):581-585.
12. Xu R, Li J, Liu J, Shi GZ, Wei K. UWB circularly polarised slot antenna with modified ground plane and L-shaped radiator. *Electron Lett.* 2018;54(15):918-919.
13. Hussain N, Jeong M, Abbas A, et al. A metasurface-based low-profile wideband circularly polarized patch antenna for 5G millimeter-wave systems. *IEEE Access.* 2020;8:22127-22135.
14. Ta S-X, Park I. Compact wideband circularly polarized patch antenna array using metasurface. *IEEE Antennas Wirel Propag Lett.* 2017;16:1932-1936.
15. Srinivasan K, Balasaraswathi M, Boopathi CS, Tran HH. Single-layer wideband circularly polarized antenna array using sequential phase feed for C-band applications. *Wirel Netw.* 2020;26(6):4163-4172.
16. Huang Y-J, Yang L, Li J, et al. Polarization conversion of metasurface for the application of wide band low-profile circular polarization slot antenna. *Appl Phys Lett.* 2016;109(5):917.
17. Zheng Q, Guo C, Ding J. Wideband and low RCS circularly polarized slot antenna based on polarization conversion of metasurface for satellite communication application. *Microw Opt Technol Lett.* 2018;60(3):679-685.
18. Chen Q, Zhang H. Dual-patch polarization conversion metasurface-based wideband circular polarization slot antenna. *IEEE Access.* 2018;6:74772-74777.
19. Liu Y, Huang Y-X, Liu Z-W, et al. Design of a compact wideband CP metasurface antenna. *Int J RF Microw Comput Aided Eng.* 2020;30(2):e22332.
20. Zhang W, Liu Y, Jia Y. Circularly polarized antenna array with low RCS using metasurface-inspired antenna units. *IEEE Antennas Wirel Propag Lett.* 2019;18(7):1453-1457.
21. Zheng Q, Guo C, Vandenbosch GAE, Ding J. Low-profile circularly polarized array with gain enhancement and RCS reduction using polarization conversion EBG structures. *IEEE Trans Antennas Propag.* 2020;68(3):2440-2445.
22. Liu Q, Chen Z-N, Liu Y, et al. Compact ultra-wideband circularly-polarized weakly coupled patch array antenna. *IEEE Trans Antennas Propag.* 2017;65(4):2129-2134.

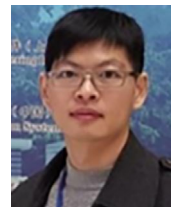
## AUTHOR BIOGRAPHIES



**Wei He** received the B.S. degree in electronic and information engineering from the Hunan University of Science and Technology, Xiangtan, Hunan, China, in 2010, and the M.S. degree in communication and information system from Shenzhen University, Shenzhen, China, in 2014, where he is currently pursuing the Ph.D. degree with the College of Electronics and Information Engineering. His current research interests include RFID tag antennas, circularly polarized antennas, and metasurface.



**Yejun He** received the Ph.D. degree in information and communication engineering from Huazhong University of Science and Technology (HUST), Wuhan, China, in 2005. Since 2011, He has been a Full Professor with the College of Electronics and Information Engineering, Shenzhen University, Shenzhen, China, where He is the Director of Guangdong Engineering Research Center of Base Station Antennas and Propagation, and the Director of Shenzhen Key Laboratory of Antennas and Propagation, Shenzhen, China. He was awarded as Pengcheng Scholar Distinguished Professor, Shenzhen, China in 2020. He was nominated as a Fellow of IET in 2016 and the Chair of IEEE Antennas and Propagation Society-Shenzhen Chapter in 2018. His research interests include wireless communications, antennas and radio frequency.



**Sai-Wai Wong** received the Ph.D. degree in communication engineering from Nanyang Technological University, Singapore, in 2009. Since 2017, he has been a Full Professor with the College of Electronics and Information Engineering, Shenzhen University, Shenzhen, China. His current research interests include RF/microwave circuit and antenna design.





**Long Zhang** received the B.S. and M.S. degrees in Electrical Engineering from the Huazhong University of Science and Technology (HUST), Wuhan, China, in 2009 and 2012, respectively, and the Ph.D. degree in electronic engineering from the University of Kent, Canterbury, U.K, in 2017. He is currently an Assistant Professor with the College of Electronics and Information Engineering, Shenzhen University, Shenzhen, China. His current research interests include circularly polarized antennas and arrays, mm-wave antennas and arrays, phased arrays, tightly coupled arrays, and reflect arrays. He is a recipient of the Shenzhen Overseas High-Caliber Personnel Level C (“Peacock Plan Award” C).



**Wenting Li** received the B.S. in electronic information engineering and the M.S. degree in electromagnetic field and microwave technology from the Northwestern Polytechnical University, Xi’an, China, in 2011 and 2014, respectively, and the Ph.D. degree in electronic engineering from the University of Kent, Canterbury, U.K, in 2019. He is currently an Assistant Professor with the College of Electronics and Information Engineering, Shenzhen University, Shenzhen, China. His current research interests include reflectarray antennas, reconfigurable antennas, circularly polarized antennas, and multibeam antennas. He is a recipient of the Shenzhen Overseas High-Caliber Personnel Level C (“Peacock Plan Award” C).



**Haixia Cui** received the M.S. and Ph.D. degrees in Communication Engineering from South China University of Technology (SCUT), Guangzhou, China, in 2005 and 2011, respectively. She is currently a Full Professor with the school of Physics and Telecommunication Engineering, South China Normal University (SCNU), China. From July 2014 to July 2015, she visited the Department of Electrical and Computer Engineering, the University of

British Columbia (UBC), as a Visiting Scholar. Her research interests are in the areas of cooperative communication, wireless resource allocation, 5G/6G, and antennas.



**Prof. Amir Boag** received the B.Sc. degree in electrical engineering and the B.A. degree in physics in 1983, both Summa Cum Laude, the M.Sc. degree in electrical engineering in 1985, and the Ph.D. degree in electrical engineering in 1991, all from Technion – Israel Institute of Technology, Haifa, Israel. From 1991 to 1992 he was on the Faculty of the Department of Electrical Engineering at the Technion. From 1992 to 1994 he has been a Visiting Assistant Professor with the Electromagnetic Communication Laboratory of the Department of Electrical and Computer Engineering at the University of Illinois at Urbana-Champaign. In 1994, he joined Israel Aircraft Industries as a research engineer and became a manager of the Electromagnetics Department in 1997. Since 1999, he is with the Physical Electronics Department of the School of Electrical Engineering at Tel Aviv University, where he is currently a Professor. Dr. Boag’s interests are in computational electromagnetics, wave scattering, imaging, and design of antennas and optical devices. He has published over 110 journal articles and presented more than 250 conference papers on electromagnetics and acoustics. Prof. Boag is an Associate Editor for IEEE Transactions on Antennas and Propagation. He is a Fellow of the Electromagnetics Academy. In 2008, Amir Boag was named a Fellow of the IEEE for his contributions to integral equation based analysis, design, and imaging techniques.

**How to cite this article:** He W, He Y, Wong S-W, et al. A low-profile ultra-wideband circularly polarized antenna array with metasurface. *Int J RF Microw Comput Aided Eng.* 2021;31(12):e22874. <https://doi.org/10.1002/mmce.22874>